Journal of Solid State Chemistry **149,** 256–261 (2000)
doi:10.1006/jssc.1999.8525, available online at http://www.idealibrary.com on IDEAL®

Crystal Growth and Structure of $AlSr_2YCu_2O_7$

P. Bordet,* F. Licci,† C. Bougerol-Chaillout,* and M. Marezio†

*Laboratoire de Cristallographie, CNRS-UJF-INPG, B.P. 166, 38042 Grenoble Cedex 9, France; and †MASPEC-Institute, CNR, Parco Area delle Scienze 37/A, 43010 Fontanini-Parma, Italy

Received July 30, 1999; in revised form September 15, 1999; accepted October 11, 1999

Millimeter-size crystals of $AlSr_2YCu_2O_7$ were synthesized by the flux method in alumina crucibles. Different mixtures of SrO : CuO (ranging from 25 : 75 to 12 : 88 mol ratio) were used as flux. No aluminum was added to the reagents. Depending on the flux composition and cooling rate, crystals different in morphology and size were obtained. The crystals appear to be tetragonal, space group *P*4/*mmm*. However, electron diffraction photographs, in agreement with Ramírez-Castellanos *et al.* (1), reveal that the symmetry is othorhombic with a cell $a = 2a_t$, $b = 4a_t$, and $c = 2c_t$ (the subscript t refers to the YBCO tetragonal cell). The structural refinement was based on X-ray data collected with a KCCD Nonius diffractometer equipped with a graphite monochromator and Ag$K\alpha$ radiation. One hundred and ninety-seven independent reflections with respect to the space symmetry quoted above, with $I > 3\sigma$, were used. The arrangement is that of a YBCO structure in which the chain Cu cations have been replaced by Al. This substitution induces the movement of the oxygen atoms in the basal layer in such a way as to form, together with the apical oxygen atoms, corner-sharing zig-zag chains of oxygen tetrahedra centered around the Al cations and running parallel to the *a*-axis either tetragonally or orthorhombically. The *b*- and *c*-axes are quadrupled and doubled, respectively, because the zig-zag chains are out of phase perpendicularly to these directions. The additional distortion results in the shift of Al to $xx0$ ($x \approx 0.056$) from 000, O1 to xxz ($x \approx 0.073$) from $00z$, and O3 to $(0.5, y, 0)$ ($y \approx 0.116$) from $(0.5, 0, 0)$.

Key Words: **Al–Sr-substituted YBCO; crystal growth; structure.**

1. INTRODUCTION

One strategy for optimizing materials of a given superconducting system may be based on cation or anion substitutions guided by crystal chemical considerations. Since high-temperature superconducting materials are multinary compounds, it is very difficult to understand how cation or anion substitution affects the local structure and in turn the physical parameters. Probable failures can be eventually understood only by precise structural studies. For example, mechanical and chemical pressures applied to the YBCO structure have the opposite effect on T_c; while the former induces increases of T_c, the latter only decreases T_c. One way to apply chemical pressure to the YBCO structure, or more generally to most of the cuprate superconductors, is to substitute Sr for Ba. This substitution induces decreases in T_c, in every cuprate except $La_{2-x}Ba_xCuO_4$. In order to understand this unexpected behavior we are carrying out a continuing program on the Sr substitution for Ba in cuprate superconductors. This article, which is part of this program, reports on the synthesis of $AlSr_2YCu_2O_7$ crystals and their structure as determined by single-crystal X-ray diffraction. The way the formula is written shows that the compound is actually YBCO in which all the chain copper and Ba cations have been replaced by Al and Sr, respectively. The Al substitution for Cu is necessary for obtaining the Sr-substituted 1212 phase under normal pressure.

The structural arrangement of $AlSr_2YCu_2O_7$ was first reported by Ramírez-Castellanos *et al.* (1). Previously, Dabrowski *et al.* (2) reported a similar compound, such as $GaSr_2YCu_2O_7$. Its structure was determined from X-ray powder diffraction data from which the authors deduced that it had the arrangement of YBCO with Ba and chain copper replaced by Sr and Ga cations, respectively. The Ga cations were placed in tetrahedral coordination with the tetrahedra forming chains parallel to one of the basal crystallographic axes, but no atomic positions were given. Ramírez-Castellanos *et al.* (1) determined the Al-1212 structure by selected area electron diffraction (SAED) and high-resolution transmission electron microscopy (HRETM). They showed that the Al cations substitute for the chain copper and, by assuming tetrahedral coordination, induce a rearrangement of the oxygen atoms in the chain-copper layers. The new ordering of the oxygen atoms induces an orthorhombic symmetry related to the tetragonal YBCO by the relationship $a = 2a_t$, $b = 4a_t$, and $c = 2c_t$ (where the subscript t indicates the YBCO tetragonal cell). The authors observed that the powder pattern could be indexed on a tetragonal cell. However, this higher symmetry was due to the average of different domains generated on going from the YBCO cell to the large one. Our electron diffraction

0022-4596/00 $35.00

studies confirmed the cell proposed by Ramírez-Castellanos *et al*. We refined the structure by single-crystal X-ray diffraction data. Even though we collected the X-ray intensities on the tetragonal cell, we were able to determine the structure in detail by allowing the atoms, exhibiting anomalously large Debye–Waller factors, to move out of the symmetry positions of the *P*4/*mmm* space group.

2. CRYSTAL GROWTH AND STOICHIOMETRY

Crystals of $AlSr_2YCu_2O_{7\pm d}$ were grown by slowly cooling off-stoichiometric melts of 99.99% Y_2O_3, CuO, and $SrCO_3$. A total of 15–20-g components was weighed, mixed and ground in an agate ball mill, under ethanol, for a few hours. The SrO:CuO mixtures, ranging from 25:75 to 12:88 mol%, used as solvents and the corresponding off-stoichiometric melt components are reported in Table 1. Note that no Al_2O_3 was included with the reagents. After drying, the mixtures were hand-pressed into 10-ml high-density alumina crucibles (Alsint 99.7). The filled crucibles were introduced into a cold Kanthal chamber furnace and slowly heated to 1080°C in air. After 24-h soaking at this temperature, the furnace was cooled in one step to 1020°C and then to 970°C at rates of 1.5–0.5°C/h. The residual liquid was absorbed by suction using a porous ceramic piece (3), and the crucible was cooled to room temperature in 10 to 15 h. Crystals could easily be removed by careful tapping the crucible walls.

Depending on the flux composition and cooling rate, crystals of different morphology and size were obtained. Al-1212 was the main phase to segregate from melts with molar SrO:CuO ratio close to the eutectic composition ($\approx$15:85) (4). The crystals typically exhibited a regular platelet shape of mm-size (2–4 mm long and < 1 mm thick) and shining surfaces. At low CuO concentration (75 mol%) Al-rich phases formed (see Table 1). At CuO concentrations higher than 85 mol%, CuO was found to be the main phase to segregate. Low cooling rates seemed to favor the crystallization of CuO with respect to the 1212 phase.

Systematic experiments on the effects of the flux composition on alumina crucible corrosion and aluminum incorporation in $YBa_2Cu_{3-x}Al_xO_{7\pm d}$ crystals were reported and discussed elsewhere (5). When Sr was used instead of Ba some differences were observed. The alumina crucible corrosion in the presence of SrO was more severe than in the case of BaO-based flux. This is probably due to two factors: the SrO–CuO mixtures melt at higher temperatures than the BaO–CuO ones, which increases the reactivity of the former with the crucible; second, Al has a higher solubility in the 1212 Sr-phase than in the corresponding Ba-phase (6). This substracts Al from the equilibrium, thus increasing the dissolution of more Al_2O_3. As observed for the BaO–CuO flux, the Al content in the crystals decreases as the flux approaches the eutectic composition. In the presence of Sr it saturates at about 1 mol Al per unit formula, which corresponds to 100% substitution of the chain Cu cations of the YBCO phase.

The cation stoichiometry was determined by energy dispersive spectroscopy (EDS) analysis using a KEVEX system attached either to a SEM (JEOL 840 operated at 30 KV) or to a TEM (Philips CM microscope operated at 300 KV) to study the surface or the bulk of the crystals, respectively. The results obtained by SEM are summarized in Table 1. Tests on different portions of the crystal surface did not reveal significant differences in the cation stoichiometry. With the exception of the first

TABLE 1
Crystal Growth and Stoichiometry Determined by EDS/SEM

	Flux (mol%)		Melt composition (cation%)				Platelet stoichiometry[a]			
Run	Sr:	Cu	Y:	Sr:	Cu	Yield (crystals)	Al:	Sr:	Y:	Cu
1	25:	75	1.25:	25.625:	73.125	few, μ-size platelets	1.32:	2.23:	0.86:	1.58
2	20:	80	1.25:	21.77:	77.75	few platelets	1.1:	2.23:	0.99:	1.68
3	19:	81	1.25:	20.075:	78.675	mm-size platelets	0.99:	2.25:	0.95:	1.73
4	18:	82	1.25:	20.075:	79.6	mm-size platelets	0.99:	2.2:	1.08:	1.73
5[b]	18:	82	1.25:	19.15:	79.6	tin platelets and CuO needles				
6[b]	17:	83	1.25:	18.225:	80.525	tin platelets and CuO needles				
7	16:	84	1.25:	17.3:	81.45	platelets and CuO needles	0.97:	2.23:	1.03:	1.77
8	15:	85	1.25:	16.375:	82.375	platelets and CuO needles	1.00:	2.18:	1.07:	1.74
9	14:	86	1.25:	15.45:	83.3	CuO needles and very few platelets				
10	12:	88	1.25:	13.6:	85.15	CuO needles				

[a] Values normalized to 6 cations per unit formula.
[b] Melts cooled at 0.5°/h. In other experiments a cooling rate of 1.5°/h was applied.

run, corresponding to an Sr-rich flux batch, the crystals exhibited similar compositions. The tests reproducibly indicated that:

— Al and Y are equimolar, each $\approx 1/6$ of the total cations.

— Sr and Cu concentrations are systematically higher and lower than 2/6, respectively.

Crystals grown from the 25 mol% SrO flux contained higher concentrations of Al and lower concentrations of Y and Cu, respectively. The Sr concentration remained constant, within the experimental error.

EDS analysis at TEM was performed on eight different grains from the same batch (run 4 in Table 1). The standards used for the quantitative analysis were $SrCuO_2$, Y_2BaCuO_5, and $Y_3Al_5O_{12}$. The molar ratios of cations in the grains were found to be Cu/Sr = 0.99(2), Cu/Y = 2.01(10), and Cu/Al = 3.34(33) (numbers in parentheses indicate the variance of the results). Such ratios approximately correspond to an $Al_{0.6}Sr_2YCu_2O_w$ stoichiometry. When compared with the SEM analysis, these results show a significant difference as far as the Al concentration is concerned. A reasonable explanation for such a discrepancy is that the crystals nucleated and grew for a relatively long time (about 2 days), during which the solution composition varied. In particular, the Al concentration in the flux increased with increasing time, due to the continuous crucible corrosion and component diffusion. A positive concentration gradient from the nucleus to the crystal surface may then be expected.

In order to account for the large concentration of Al vacancies, we considered the possible substitution of Al by C as a CO_3^{-2} carbonate group. The qualitative infrared spectrum, taken by a Fourier-transform IR spectrometer (FTIR) on a sample comprising a few crystals, however, did not reveal the presence of such groupings. They could only be present at a very low concentration. In any case this hypothesis would not explain the small Debye–Waller factor yielded by the structural refinement (see below).

3. X-RAY INTENSITY DATA COLLECTION AND STRUCTURAL REFINEMENTS

The X-ray intensities were measured by a KCCD Nonius diffractometer equipped with a graphite monochromator and Ag$K\alpha$ radiation. The crystal-to-detector distance was 26.5 mm at $\theta = 0$. The sample was a platelet-like crystal (4 in Table 1) whose dimensions had been reduced and about equalized by the use of a diamond-walled grinder. Ninety frames were scanned every 2° in ϕ, each for a period of 2 min. This procedure and extending the measurements to $\sin\theta/\lambda = 0.714$ yielded 1873 reflections. The reflections as recorded on the detector were integrated and converted to I by the Denzo-SMN program (7). The absorption correction ($\mu = 167.4\ cm^{-1}$) was applied by the use of the program SORTAV (8). By averaging over the tetragonal point symmetry 4/*mmm*, 199 independent reflections were obtained, which were reduced to 197 by the cutoff $I > 3\sigma$.

TABLE 2
Positional, Thermal, and Occupancy Parameters of $AlSr_2YCu_2O_7$

	Occupancy	x	y	z	$U11$	$U22$	$U33$
Al	0.25	0.056(1)	0.056	0.0	0.000(2)		
Sr	1.0	0.5	0.5	0.19332(9)	0.0212(5)		0.0116(7)
Y	1.0	0.5	0.5	0.5	0.0059(5)		0.0093(7)
Cu2	1.0	0.0	0.0	0.3492(1)	0.0042(5)		0.0130(8)
O1	0.25	0.073(3)	0.073	0.140(1)	0.037(5)		
O2	1.0	0.5	0.0	0.3653(5)	0.005(2)	0.014(2)	0.026(2)
O3	0.25	0.5	0.116(6)	0.0	0.040(6)		

The structure was refined by using the MXD program (9). The initial model corresponded to the structure of $CuSr_2YCu_2O_7$ with the Cu chain cations at 000 replaced by Al and the mobile oxygen at 0.500. This refinement clearly indicated that the block containing the layers AlO and SrO was disordered. The temperature factors of the Al cations and those of the oxygen atoms, O1 and O3, of the AlO and SrO layers, respectively, were anomalously large. In the following cycles the Al cations were placed in the $xx0$ positions while the O1 and O3 were placed in the xxz and $0.5y0$ positions, respectively, and the new parameters, x_{Al}, x_{O1}, and y_{O3} were allowed to vary toghether will all the other variable parameters, including that corresponding to the extinction correction. During the last cycles of refinement the anisotropic temperature factors for the Y, Sr, and Cu2 cations were introduced, while the temperature factors of the oxygen and Al atoms were kept isotropic. The final R factors were 0.042 (weighted) and 0.029 (unweighted) with

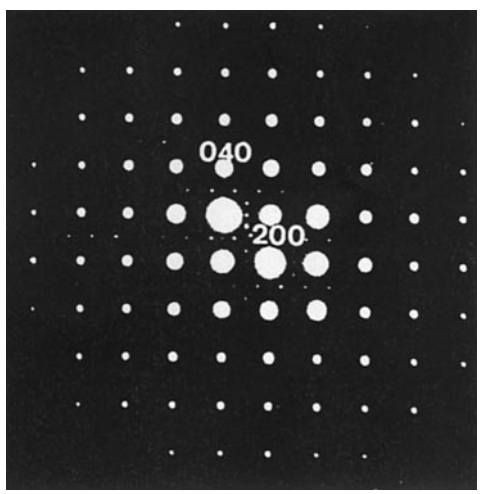

FIG. 1. Electron diffraction pattern along the [001] zone axis of $AlSr_2YCu_2O_7$. The indices are given in the $2a_t \times 4a_t$ supercell.

$\chi^2 = 1.15$. The final positional and thermal parameters are reported in Table 2.

It should be noticed that the thermal parameter of the Al cation is practically zero. This indicates that either the displacement from 000 to $xx0$ does not take into account completely the disorder existing in that position or a heavier cation than Al is partially occupying the position. The EDS analysis, however, demonstrated that the crystals do not contain an excess of copper with respect to the formula $AlSr_2YCu_2O_7$. We then assumed that the positions around 000 are occupied entirely by Al cations, and the small value of their thermal parameter is due to an additional disorder or modulation which is not taken into account by the present model.

4. ELECTRON DIFFRACTION STUDY

Electron diffraction patterns taken along the [001] zone axis show the presence of superstructure reflections beside the basic tetragonal ones corresponding to $a_t \times a_t$ (Fig. 1).

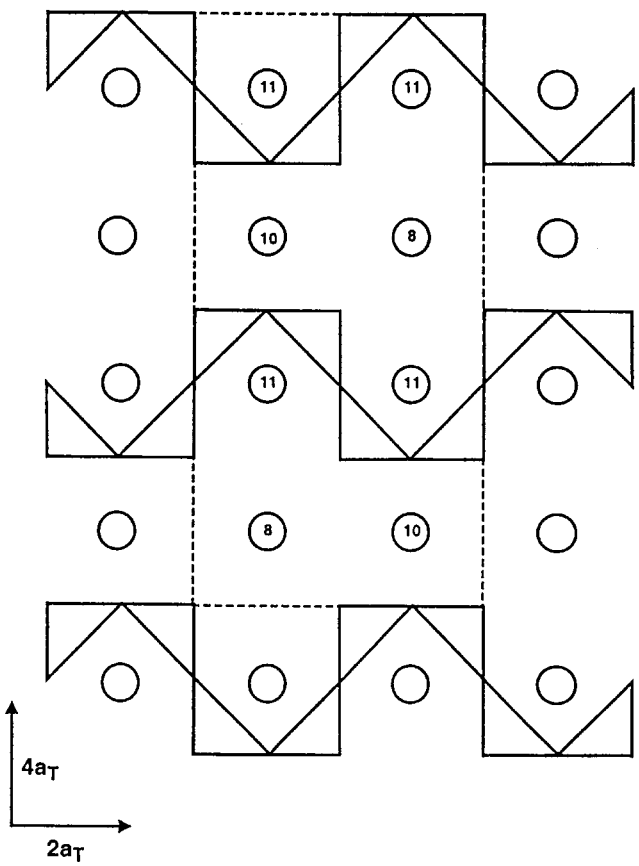

FIG. 2. Schematic representation of the zig-zag corner-sharing AlO_4 tetrahedral chains running along the $2a_t$ axis. The circles represent the Sr cations. The numbers inside the circles give the oxygen coordination for the specific site. Each Sr cation has four oxygen neighbors located on the CuO_2 layers just above the SrO layer.

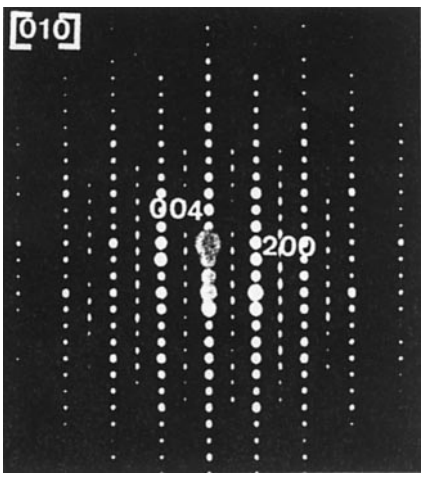

FIG. 3. Electron diffraction pattern along the [010] zone axis of $AlSr_2YCu_2O_7$. The indices are given in the $2a_t \times 2c_t$ supercell. One notices the presence of a diffuse line parallel to c^* and passing through the supercell reflections.

To be indexed these extra reflections require an orthorhombic $2a_t \times 4a_t$ unit cell (where the subscript t refers to the basic tetragonal cell), as proposed by Ramírez-Castellanos *et al.* (1), and the presence of domains rotated by 90° with respect to each other. In the supercell the extinction rule is $h + k = 2n$ for $hk0$, indicating a centering of the chain arrangement in the basal plane, in agreement with the model proposed in Fig. 2. The orthorhombic cell would be due to the zig-zag configuration of the chains along the a-axis and the out-of-phase position of the parallel ones.

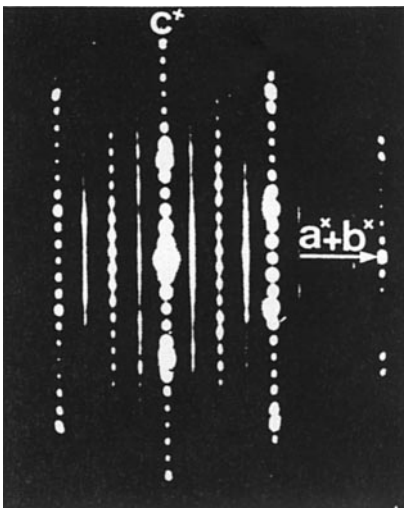

FIG. 4. Electron diffraction pattern along the [110] zone axis of $AlSr_2YCu_2O_7$ in the $2a_t \times 4a_t \times 2c_t$ supercell. Diffusion lines parallel to c^* and joining the superstrucure reflections are clearly visible.

Along the [010] zone axis (Fig. 3), the superstructure reflections are present at $h0l$ positions in a $2a_t \times 2c_t$ cell with the condition $h + l = 2n$. The doubling of the c-axis can again be explained by the out-of-phase configuration of successive chains along c. Depending on the crystallites, these superstructure reflections are more or less elongated along c^*, indicating a lack of correlation between successive blocks of ordered chains. In some cases, continuous diffuse lines parallel to c^* have been observed (Fig. 4) in photographs taken along the [110] zone axis.

5. DESCRIPTION OF THE STRUCTURE

The structural arrangement of $AlSr_2YCu_2O_7$ is that of YBCO in which the chain Cu cations have been replaced by Al. The latter cations, preferring the tetrahedral coordination, induce the oxygen atoms of the basal layer to move, creating the tetrahedral environment around the 000 positions. As schematized in Fig. 2, the O3 atoms at 1/2,0,0 of every other row parallel to the a-axis of the orthorhombic YBCO cell move to the 0,1/2,0 positions. The additional distortion of the O3 sublattice to the positions (1/2,0.119,0) and (0.119,1/2,0), along with that of O1 to (0.082,0.082,0.1369) and that of Al to (0.068,0.068,0), is needed to generate more regular tetrahedra. As shown in Fig. 5, the tetrahedra form one-dimensional zig-zag corner-sharing chains running along the a-axis. These chains are responsible for the doubling of the basal axes. Moreover, it has been shown by Ramírez-Castellanos *et al.* (1) and confirmed by us that in some of the electron diffraction patterns the b-axis is actually multiplied by 4, which indicates that the chains are out of phase along the a-axis with respect to each other. Since the c-axis is also doubled, the chains are out of phase also along c. The average O–Al–O angle is 108.7° with an average deviation of 12°. The average Al–O distance is 1.75 Å, which is shorter than that calculated from the Shannon ionic radii (1.79 Å) (10) (See Table 3.). This discrepancy is probably due to the averaging of the orthorhombic domains, resulting in a tetragonal symmetry from which it is difficult to extract the total distortion.

As shown in Fig. 2 and according to the $2a \times 4a \times 2c$ cell, there are three types of Sr sites in the structure. Two of them are fourfold and one is eightfold. The two fourfold sites are 8- and 10-coordinated, respectively, while the eightfold site is 11-coordinated. The average distances are 2.56, 2.86, and 2.90 Å, respectively. If these are compared to the distances calculated from the Shannon ionic radii (10), one finds that

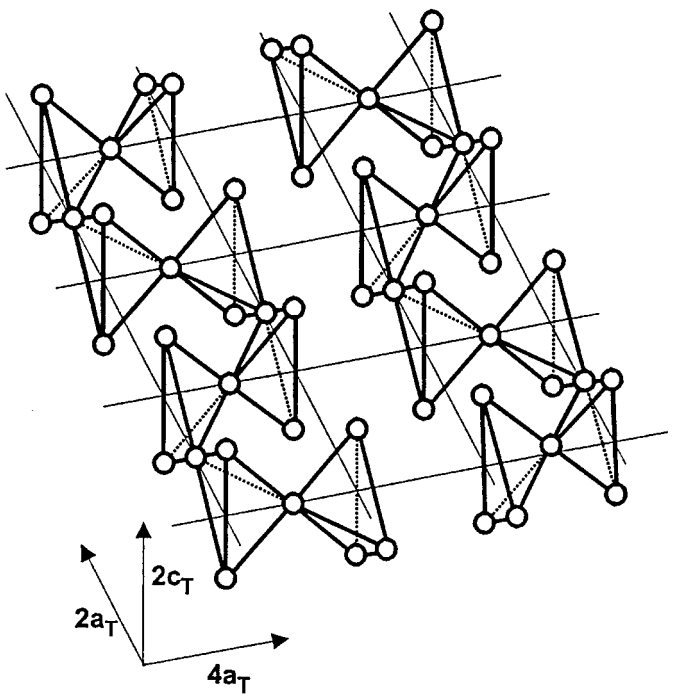

FIG. 5. A three-dimensional schematic representation of the zig-zag corner-sharing AlO_4 tetrahedral chains. Along the $4a_t$ axis the chains are out of phase, the feature responsible for the quadrupling of the axis.

TABLE 3
Selected Interatomic Distances (Å) and Angles (°)

Al–O1	1.73(1) × 2
Al–O3	1.82(1)
Al–O3	1.678(8)
Average	1.74 (from Shannon 1.79)
O1–Al–O1	123.7°
O1–Al–O3	111.8 × 2
O1–Al–O3	100.0 × 2
O1–Al–O3	106.7
Average	109.0
8-coordinated Sr	
Sr–O1	2.365(9) × 4
Sr–O2	3.216(4) × 4
Average	2.545
10-coordinated Sr	
Sr–O1	2.835( ) × 4
Sr–O2	2.725( ) × 4
Sr–O3	3.216( ) × 2
Average	2.867
11-cordinated Sr	
Sr–O1	3.237( ) × 2
Sr–O1	2.835( ) × 2
Sr–O2	2.725( ) × 4
Sr–O3	2.608( ) × 1
Sr–O3	3.216( ) × 2
Average	2.917
Y–O2	2.443(3) (from Shannon 2.41)
Cu–O2 (planar)	1.9378(5)
Cu–O1 (apical)	2.41(1)
Average	2.03

the 8-coordinated is too short by about a tenth of an Ångstrom while the other two are too long by the same amount.

The other two cation–oxygen distances, namely, Cu–O and Y–O, which are inside the block $(CuO_2)(Y)(CuO_2)$ are less affected by the rearrangement of the oxygen atoms of the basal layer and of the apical oxygen. They agree well with those found in the YBCO structures. Note that the apical Cu2–O distance is rather short (2.37 Å) for an insulating YBCO compound. It is well known that in this class of compounds the so-called apical distance scales well with the metallic behavior of YBCO and eventually with T_c (11, 12). The value of this distance was found to vary from 2.48 Å for insulating $YBa_2Cu_3O_6$ to 2.28 Å for $YBa_2Cu_3O_7$. Its variation, besides its scaling well with the metallic behavior and T_c, revealed that a charge transfer takes place from the chain to the planar copper, when the oxygen content varies between O_6 and O_7. In $AlSr_2YCu_2O_7$ the Al, Sr, Y, and Cu cations are in the $3+$, $2+$, $3+$, and $2+$ state, respectively; thus no cation is in a mixed valence state, and consequently the oxygen content is fixed at 7 and no charge transfer can take place. However, it should be pointed out that the apical distance in the Al–Sr compound is 2.37 Å, which in the YBCO system corresponds to $YBa_2Cu_3O_{6.5}$, a metallic and 60 K superconducting compound.

ACKNOWLEDGMENTS

The authors thank P. Ferro for the assistance in the crystal growth, T. Fournier for the EDS-SEM analysis, and C. Mucchino for the FTIR test.

REFERENCES

1. J. Ramírez-Castellanos, Y. Matsui, M. Ysobe, and E. Takayama-Muromachi, *J. Solid State Chem.* **133,** 434 (1997).
2. B. Drabowski, P. G. Radaelli, D. G. Hinks, A. W. Mitchell, J. T. Vaughey, D. A. Groenke, and K. R. Poeppelmeier, *Physica C* **193,** 63 (1992).
3. R. Boutellier, B. N. Sun, H. J. Scheel, and H. Schmid, *J. Crystal Growth* **96,** 465 (1989).
4. R. S. Roth, C. J. Rawn, J. D. Whitler, C. K. Chiang, and W. K. Wong-Ng, *J. Am. Ceram. Soc.* **72,** 395 (1989).
5. F. Licci, C. Frigeri, and H. J. Scheel, *J. Crystal Growth* **112,** 606 (1991).
6. T. Den and T. Kobayashi, *Physica C* **196,** 141 (1992).
7. Z. Otwinowski and W. Minor, "Methods in Enzymology" (C. W. Corter, Jr., and R. M. Sweet, Eds.), Vol. 276. Academic Press, San Diego, 1996.
8. R. H. Blessing, *Acta Crystallogr.* **A51,** 33 (1995).
9. P. Wolfers, *J. Appl. Crystallogr.* **23,** 554 (1990).
10. R. D. Shannon, *Acta Crystallogr.* **B32,** 751 (1976).
11. R. J. Cava, A. W. Hewat, E. A. Hewat, B. Batlogg, M. Marezio, K. M. Rabe, J. J. Krajewski, W. F. Peck, Jr., and L. W. Rupp, Jr., *Physica C* **165,** 419 (1990).
12. J. D. Jorgensen, B. W. Veal, A. P. Paulikas, L. J. Nowicki, G. W. Crabtree, H. Claus, and W. K. Kwok, *Phys. Rev. B* **41,** 1863 (1990).